AEM
Journals.ASM.org

TiO_2 Photocatalysis Damages Lipids and Proteins in *Escherichia coli*

Gaëlle Carré,[a,b] Erwann Hamon,[c*] Saïd Ennahar,[c] Maxime Estner,[a] Marie-Claire Lett,[d] Peter Horvatovich,[e] Jean-Pierre Gies,[a] Valérie Keller,[b] Nicolas Keller,[b] Philippe Andre[a]

Laboratoire de Biophotonique et Pharmacologie, UMR 7213 CNRS and Strasbourg University, Illkirch, France[a]; Institut de Chimie et Procédés pour l'Energie, l'Environnement et la Santé (ICPEES), UMR 7515 CNRS and Strasbourg University, Strasbourg, France[b]; Laboratoire de Chimie Analytique des Molécules BioActives, UMR 7178 CNRS and Strasbourg University, Illkirch, France[c]; Laboratoire de Génétique Moléculaire, Génomique, Microbiologie, UMR 7156 CNRS and Strasbourg University, Strasbourg, France[d]; Department of Analytical Biochemistry, Center of Pharmacy, Groningen University, Groningen, The Netherlands[e]

This study investigates the mechanisms of UV-A (315 to 400 nm) photocatalysis with titanium dioxide (TiO_2) applied to the degradation of *Escherichia coli* and their effects on two key cellular components: lipids and proteins. The impact of TiO_2 photocatalysis on *E. coli* survival was monitored by counting on agar plate and by assessing lipid peroxidation and performing proteomic analysis. We observed through malondialdehyde quantification that lipid peroxidation occurred during the photocatalytic process, and the addition of superoxide dismutase, which acts as a scavenger of the superoxide anion radical ($O_2{\cdot}^-$), inhibited this effect by half, showing us that $O_2{\cdot}^-$ radicals participate in the photocatalytic antimicrobial effect. Qualitative analysis using two-dimensional electrophoresis allowed selection of proteins for which spot modifications were observed during the applied treatments. Two-dimensional electrophoresis highlighted that among the selected protein spots, 7 and 19 spots had already disappeared in the dark in the presence of 0.1 g/liter and 0.4 g/liter TiO_2, respectively, which is accounted for by the cytotoxic effect of TiO_2. Exposure to 30 min of UV-A radiation in the presence of 0.1 g/liter and 0.4 g/liter TiO_2 increased the numbers of missing spots to 14 and 22, respectively. The proteins affected by photocatalytic oxidation were strongly heterogeneous in terms of location and functional category. We identified several porins, proteins implicated in stress response, in transport, and in bacterial metabolism. This study reveals the simultaneous effects of $O_2{\cdot}^-$ on lipid peroxidation and on the proteome during photocatalytic treatment and therefore contributes to a better understanding of molecular mechanisms in antibacterial photocatalytic treatment.

Several disinfection strategies exist, some of them involving, for example, the use of silver (1–3) or copper metal ions (4). However, the development of new disinfection approaches is required due to the rapid adaptation of bacteria and development of strains resistant to these metals (5). Among these new disinfection approaches, photocatalysis is a promising technique which belongs to advanced oxidation processes (AOP), characterized by the production of reactive oxygen species (ROS) (6). In 1985, Matsunaga et al. were the first to report on the killing of microbial cells in water by near-UV-light-irradiated platinum-loaded titanium dioxide (TiO_2) semiconductor particles (7). This pioneering work gave rise to much research in the field of disinfection by oxidative photocatalysis (8–10), with applications now found in many fields of disinfection (11, 12).

Among the various semiconductor photocatalysts studied, the wide-band-gap TiO_2 in anatase crystalline form is the most attractive one. This material has high photocatalytic efficiency due to its high quantum yield, has high stability toward photocorrosion and chemicals, is insoluble in water, and has a low toxicity and low costs. The band gap energy of 3.2 eV for TiO_2 requires photoexcitation wavelengths less than ca. 385 nm, corresponding to an irradiation with near-UV light (13).

Activation of the TiO_2 semiconductor particle with adequate UV-A light (315 to 400 nm) generates electrons and holes in the conduction and valence bands, respectively. The photogenerated charges take part in reduction and oxidation reactions at the particle surface (12, 14). In particular, holes and electrons are, respectively, reacting with adsorbed water and dioxygen molecules to form ROS, such as the ·OH hydroxyl radical and the $O_2{\cdot}^-$ superoxide radical anion, respectively. Singlet oxygen ($^1O_2$) or hydrogen peroxide (H_2O_2) can also be formed (15). The analogy between chemical and biological targets results from the organic nature of the microorganism constituents, which can react with the active surface species issued from TiO_2 photoactivation. The resulting reactions are similar to the oxidation reactions taking place at the surface of irradiated TiO_2 photocatalysts with organic molecules, e.g., during potabilization or depollution oxidative processes in water and air treatments (16).

These ROS are thus responsible for the oxidation of many organic constituents of the microorganisms (17), such as lipid peroxidation (18), protein alteration (19), or DNA damage (20). Direct contact between the targeted microorganisms and the TiO_2 particles is reported to be one of the key parameters of photocatalytic disinfection (17, 21). Notably, several transmission electron microscopy analyses revealed that the binding of *Escherichia coli* to TiO_2 particles induces cell disruption and cell debris (22–24). However, the precise molecular mechanism remains unclear and is a matter of debate.

E. coli, a Gram-negative bacterium whose complete genome has been sequenced (25), represents a suitable bacterial model to

Received 4 December 2013 **Accepted** 6 February 2014
Published ahead of print 14 February 2014
Editor: J. L. Schottel
Address correspondence to Gaëlle Carré, carregaelle1@gmail.com, or Nicolas Keller, nkeller@unistra.fr.
* Present address: Erwann Hamon, Aérial, Parc d'Innovation, Illkirch, France.

doi:10.1128/AEM.03995-13

study the antimicrobial effects of photocatalysis at a molecular level.

This paper investigates the antibacterial effect of TiO_2 photocatalysis on *E. coli* and is focused on the identification of the induced photocatalytic damage of both lipids and proteins, which are key cellular components of bacteria. Both lipid peroxidation and *E. coli* proteome modifications have been investigated in this study. Implication of the $O_2\cdot^-$ superoxide radical in lipid peroxidation has been demonstrated, and the identification of proteins of the *E. coli* ATCC 8739 strain modified by the photocatalytic treatment, performed through two-dimensional electrophoresis (2-DE), may offer insights into the mechanism behind the antibacterial effects of TiO_2.

MATERIALS AND METHODS

Bacterial strains and growth media. Before each experiment, one loopful of *Escherichia coli* strain ATCC 8739 was seeded on a slant of tryptic soy agar (TSA) (Bio-Rad) and grown aerobically at 37°C for 24 h. The bacterial inoculum was monitored by setting the culture optical density at an absorbance wavelength of 620 nm (OD_{620}), at 0.156, corresponding to 10^8 CFU/ml.

Photocatalytic material. Experiments were performed with commercial TiO_2 Aeroxide P25 (Evonik, Frankfurt, Germany, 20% rutile–80% anatase crystalline form, with a specific surface of 50 m^2/g).

Photocatalytic experimental setup. The photocatalytic tests have been assessed using an experimental setup composed either of a 96-well plate—each well acting as a single liquid-phase photocatalytic reactor—for determining cell viability on agar plates or of petri dishes for both lipid and proteomic analyses, since they require large amounts of materials. In each case, different amount of TiO_2 were added in a range from 0.1 to 0.8 g/liter. The photocatalytic device is composed of four equidistant commercial BlackLight Blue lamps (BLB) (40 W; Actinic, Philips, Eindhoven, The Netherlands) with a spectral peak centered on 365 nm and providing an irradiance of 30 W/m^2 to the wells or petri dishes. After addition of the bacteria and TiO_2 to the photocatalytic reactor, UV-A irradiation starts immediately for two 96-well plates, with an exposure time of 30 min or 60 min; one other 96-well plate stayed in the dark for the same durations. All the 96-well plates were placed on a shaker (Heidolph Duomax 1030) operating at 40 rpm to ensure adequate mixing and contact between TiO_2 particles and bacteria. The pH of the photocatalytic suspensions at the end of the experiment was 7.8. Each experimental condition with respect to test duration and TiO_2 concentration corresponded to a single well and was performed in triplicate.

Cell viability measurement. *E. coli* was grown at 37°C in Mueller-Hinton (MH) broth (Bio-Rad) until the culture reached an OD_{620} of 0.156, corresponding to 1×10^8 CFU/ml. After centrifugation at 9,000 × *g* for 10 min, the supernatant was removed and the bacterial pellet was resuspended in sterile physiological water (NaCl, 9 g/liter) to obtain 10^8 CFU/ml. This population was diluted to obtain an inoculum of 1×10^6 CFU/ml. Each photocatalytic well reactor (96-well plate) was filled with 90 μl of 10^6-CFU/ml bacterial suspensions to which 10 μl of a TiO_2 suspension in physiological water was added for the tests, with TiO_2 concentrations of 0.1 g/liter, 0.2 g/liter, 0.4 g/liter, and 0.8 g/liter. The tests were carried out with or without TiO_2. After the different treatments, dilutions were made in physiological water, and 100 μl (each) of the resulting solutions were spread on TSA. Each agar plate was incubated at 37°C for 24 h, and bacteria were counted after incubation.

The logarithm of reduction, i.e., $\log_{10}(C/C_0)$, where C_0 is the concentration of control live bacteria without TiO_2 in the dark, expressed in CFU/ml, and C is the concentration of live bacteria for other conditions, expressed in CFU/ml, was determined.

Lipid oxidation. The thiobarbituric acid (TBA) assay (OxiSelect TBA reactive substances [TBARS] assay kit; Euromedex, Strasbourg, France) was used and was slightly modified by increasing the bacterial population to assess the lipid peroxidation state. TBA reacts at 95°C with malondialdehyde (MDA). MDA is a lipid oxidation product and provides a colored MDA-TBA adduct. The concentration of this adduct can be derived by measuring the absorbance at 532 nm by spectrophotometry.

E. coli was grown at 37°C in 1,500 ml Mueller-Hinton (MH) broth (Bio-Rad) until the culture reached an OD_{620} of 0.156 (~1×10^8 CFU/ml). After centrifugation at 9,000 × *g* for 10 min, the supernatant was removed and the bacterial pellet was resuspended in 150 ml of physiological water to obtain a final population of 1×10^9 CFU/ml. Fifty milliliters of this suspension, containing 5×10^{10} CFU, was divided into 5 petri plates of 10 ml (each) and further used as a photocatalytic reactor. In fact, this lipid quantification kit is designed for eukaryotic cells, and prokaryotic cells required larger amounts of bacteriologic materials. The petri dishes containing 0.4 g/liter of TiO_2 were placed on a shaker plate operating at 40 rpm (Heidolph Duomax 1030) during the 60 min of UV-A irradiation. Control samples were treated the same way in the dark without the TiO_2 catalyst. To demonstrate the effect of $O_2\cdot^-$ in lipid oxidation, superoxide dismutase (SOD) (1,000 U; Sigma-Aldrich, Saint Quentin Fallavier, France) was added to the reaction media before the photocatalytic treatments. To quantify lipid oxidation, the 50-ml content of each petri dish was collected and subsequently centrifuged at 9,000 × *g* for 10 min. This was followed by resuspension of bacterial pellets in 500 μl phosphate-buffered in saline. Then, 5 μl butylated hydroxyl toluene (100×) antioxidant was added to 500 μl of sample to prevent any further lipid oxidation. Finally, 250 μl of TBA reagent and 100 μl of SDS lysis buffer were added to 100 μl of sample and to MDA standards as described in the TBARS assay kit protocol. Reactions were carried out in duplicate. Then, samples and standards were kept at 95°C for 1 h, before the final centrifugation at 1,000 × *g* for 15 min took place, and the resulting supernatant was transferred to a 96-well plate to record the absorbance at 532 nm by spectrophotometry. The quantity of peroxidized lipid in milligrams was calculated with the help of the previously determined MDA standard curve.

Comparative proteomic analysis. As with lipid oxidation, proteomic analysis requires a large amount of materials. Therefore, photocatalytic tests were performed using petri plates as a reactor under vigorous stirring. After 18 h of growth of *E. coli* at 37°C on a slant of TSA, bacterial suspensions in physiological water were adjusted to an OD_{620} of 0.156 (~1×10^8 CFU/ml). Twenty milliliters of the bacterial suspension of 1×10^8 CFU/ml was divided into 2 petri dishes, used as the reactor. The proteomic analysis was performed with fresh cells and with cells subjected to 30 min of irradiation with UV-A light using 0.1 g/liter and 0.4 g/liter TiO_2. During the experiments, plates were shaken with a shaker plate at 40 rpm (Heidolph Duomax 1030). Comparisons were performed with cells treated with the TiO_2 catalyst and kept in the dark (no irradiation) and with cells subjected to UV-A light exposure in the absence of any TiO_2 catalyst. A control experiment was carried out without TiO_2 in the dark. For analysis, cells obtained after sampling were first centrifuged (3,000 × *g*, 5 min, at 4°C), and their whole proteomes were subsequently extracted by cryogrinding and purified using Trizol reagent (Euromedex, France), as previously reported by E. Hamon et al., and separated by two-dimensional electrophoresis (2-DE), with a pI range of 4.0 to 7.0 and a mass range of 10 to 250 kDa (26). Under these conditions, the estimated coverage of the theoretical proteome of *E. coli* ATCC 8739 was 62%, as inferred from an *in silico* analysis of *E. coli* protein sequence data obtained from NCBI (data not shown). Image analysis of the 2-DE gels was performed using the PD Quest 8.0.1 software program (Bio-Rad). For each condition, the same experiments were carried out in triplicate, and only spots that disappeared on the three gels were selected for intercondition comparison. Spot intensities were normalized to the sum of intensities of all valid spots in one gel. Protein expression differences were identified between different operating conditions. Only proteins present in samples of one condition and absent in one other were considered in this analysis.

Spots of interest were subjected to tryptic in-gel digestion and analyzed by chip-liquid chromatography-quadrupole time of flight (chip-

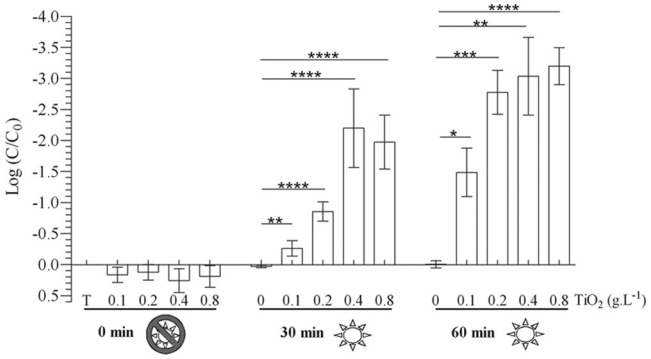

FIG 1 Influence of photocatalytic treatment on *E. coli* cell viability, determined by counting on agar plate. Bars indicate standard deviations. ◉, in the dark; ☼, under UV-A irradiation. * ($P < 0.05$), ** ($P < 0.01$), *** ($P < 0.001$), and **** ($P < 0.0001$) indicate the significance of the difference between sample means, obtained using Student's *t* test.

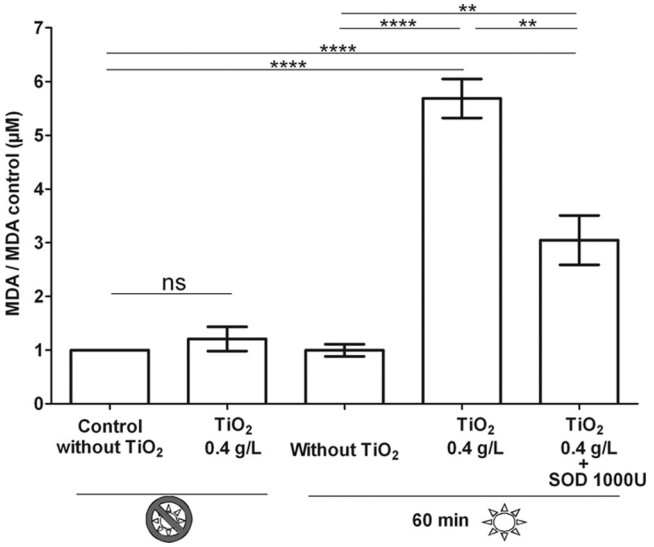

FIG 2 Impact of UV-A photocatalysis with TiO_2 and influence of the addition of SOD at 1,000 U on *E. coli* lipid peroxidation. A duration of 60 min and a TiO_2 concentration of 0.4 g/liter were chosen. Membrane lipid peroxidation is measured by assessing production of malondialdehyde (MDA). MDA is a biomarker of lipid peroxidation and is used to measure the lipid peroxidation rate relative to controls (MDA concentration obtained without and with treatment). Bars indicate standard deviations. ◉, in the dark; ☼, under UV-A irradiation. ** ($P < 0.01$), **** ($P < 0.0001$), and ns (not significant) indicate the significance of the difference between sample means obtained with Student's *t* test.

LC-QTOF) mass spectrometry using an Agilent G6510A QTOF mass spectrometer equipped with an Agilent 1200 Nano LC system and an Agilent high-performance liquid chromatography (HPLC) G4240A chip cube (Agilent Technologies, Santa Clara, CA, USA), as described previously by E. Hamon et al. (26). After data acquisition, files were uploaded to the in-house-installed version of Phenyx (Geneva Bioinformatics, Geneva, Switzerland) to search the NCBInr (r. 20110608) database with the following criteria: taxonomy: *E. coli*; scoring model, electrospray ionization (ESI)-QTOF; parent charge, +2, +3 (trust = medium); single round; methionine oxidation, cysteine carboxyamidomethylation (cysteine treated with iodoacetamide), and phosphorylation as partial modifications; trypsin as a digestion enzyme; allowance of two missed cleavages; cleavage mode, normal; parent ion tolerance, 0.6 Da; peptide thresholds, length, ≥6; score threshold, ≥5.0; identification significance, *P* value ≤ 1.0×10^{-4}; accession number score threshold, 6.0; coverage threshold, ≥0.2; identified ion series, b, b++, y, y++; and allowance of conflict resolution. A publicly available tandem mass spectrometry (MS/MS) search algorithm (open mass spectrometry search algorithm, OMSSA [27]) was used with the same search criteria described above to confirm protein identities and limit the risk of false positives. On the basis of consensus scoring, only proteins recognized by both database search algorithms at a false-positive rate of 5% were considered to be correctly identified (28).

Statistical analysis. Statistical analysis was performed using the software program Prism 5 (GraphPad Software) and was based on Student's *t* test.

RESULTS

Evidence of bacterial inactivation by UV-A-irradiated TiO_2. Figure 1 shows the influence of the different applied treatments on the viability of *E. coli* cells, determined by bacterial counting on agar plates and expressed in terms of logarithmic reduction. First, the sole application of UV-A light in the absence of TiO_2 did not caused any reduction in cell viability. Second, independently of the TiO_2 concentration within the 0.1- to 0.8-g/liter range, no cytotoxic effect of TiO_2 was observed in the dark, whereas a reduction of cell viability was observed only in samples irradiated with UV-A light and in the presence of TiO_2. This reduction was directly dependent on the duration of UV-A irradiation, since, e.g., the reduction increased from 1 to 3 logs for a TiO_2 concentration of 0.2 g/liter when the duration of UV-A exposure increased from 30 min to 60 min. Similarly, a stronger diminution of cellular viability was observed at higher TiO_2 concentrations up to 0.4 g/liter, for which a 2-log reduction was recorded for an irradiation of 30 min. However, the antibacterial effect was not increased at the higher TiO_2 concentration of 0.8 g/liter independently of the duration of UV-A exposure. This is in agreement with the usual activity pattern observed in photocatalysis applied to the oxidative degradation of organic molecules, for which the reaction rate is reported to be proportional to the mass of the catalyst before achieving a plateau. This plateau corresponds to the maximum amount of TiO_2 in which all the particles are completely illuminated (29, 30). For larger TiO_2 concentrations, a screening effect of excess particles occurs, so that part of the photosensitive surface is masked. Based on our method, counting the bacteria grown on agar plates, the highest reduction in cellular viability recorded for the studied *E. coli* strain was around 3 logs for an irradiation of 60 min in the presence of TiO_2 (0.4 g/liter).

Impact of TiO_2 photocatalysis and effect of ROS in lipid peroxidation. As shown in Fig. 2, neither TiO_2 at a concentration of 0.4 g/liter in the dark or UV-A light irradiation for 60 min without TiO_2 significantly increased lipid peroxidation. In contrast, the samples subjected to UV-A irradiation for 60 min with the presence of the TiO_2 catalyst at 0.4 g/liter produced 5.7 times more lipid peroxides than the bacterial population exposed only to UV-A irradiation for 60 min. The addition of SOD (1,000 U), known to act as a ROS scavenger selective toward the $O_2{\cdot}^-$ superoxide radical anion, partially decreased the lipid peroxidation ratio from, 5.7 to 3.0, corresponding to a 48% lipid peroxidation rate. Therefore, SOD inhibition of the $O_2{\cdot}^-$ produced by irradiated TiO_2 induced a half-diminution of lipid peroxidation. This is in agreement with our previous work, which showed that scavenging the $O_2{\cdot}^-$ superoxide radical by adding the SOD enzyme completely restored cell viability (31).

Impact of TiO_2 photocatalysis on *E. coli* whole-cell proteome. To provide a better understanding of the antibacterial mechanism of TiO_2 photocatalysis, the proteome of *E. coli* ATCC 8739 was investigated using 2-DE under different conditions. Bacterial suspensions were maintained for 30 min in the dark or under UV-A radiation without TiO_2 or with 0.1 or 0.4 g/liter of TiO_2. The duration under UV-A and TiO_2 concentration were chosen to obtain sublethal stress according to our previous work (31). Indeed, we have previously shown by cytometry that no significant modification of membrane integrity was observed for those TiO_2 concentrations in the dark or under UV-A light. In contrast, cell counts on agar plates showed that 30 min of UV-A irradiation with the presence of 0.4 g/liter TiO_2 induced a 2-log reduction in living bacteria, while membrane integrity was not affected significantly. This suggests a heterogeneous bacterial population, composed of live cells and viable but nonculturable (VBNC) cells, where VBNC indicates sublethal stress (32). However, the conserved membrane integrity indicates that both kinds of cells still conserved their whole protein machinery, allowing the comparative proteomic analysis.

In order to identify the putative protein targets of TiO_2 and UV-A irradiation-mediated oxidative stress, proteomic patterns of bacteria with different treatments (Fig. 3B to F) and a control (a sample without TiO_2 in the dark; Fig. 3A) were recorded. Proteins affected by treatment were found by identifying spots that were observed exclusively in samples under one condition but were absent under the other condition. These discriminatory spots were labeled with white (absent) and black (present) numbers in the image of 2-DE gels corresponding to treatment conditions. The proteins underlying the detected discriminatory gel spots were identified by database searches using the Phenyx and OMSSA tools. The different treatments resulted in 22 spots which disappeared in the treated samples compared to the control. Table 1 lists 21 different proteins corresponding to 22 spots, since one protein (DNA starvation/stationary-phase protection protein [Dps]) was identified in two spots (spots 12 and 13), suggesting the presence of protein isoforms.

First, Fig. 3B shows that UV-A irradiation alone led to the disappearance of a single spot (unnamed outer membrane protein [FadL]; spot 1) compared to the control (Fig. 3A), which protein is implied in lipid transport and metabolism.

The amount of protein degradation was dependent on the TiO_2 concentration in samples containing the TiO_2 catalyst but which were not exposed to UV-A irradiation. Indeed, Fig. 3C shows that 7 spots disappeared at a TiO_2 concentration of 0.1 g/liter (FadL, spot 1; outer membrane protein OmpW [OmpW], spot 5; hypothetical protein YgiW [YgiW], spot 7; H^+ ATPase F1 alpha subunit [AtpA], spot 10; indigoidine synthase A-like protein [IndA-like], spot 16; DnaK suppressor [DnaK], spot 18; small ribosomal protein S6 [ribosomal_S6], spot 19), while 19 spots disappeared at a TiO_2 concentration of 0.4 g/liter (Fig. 3E). This corresponded to 12 additional spots and 11 additional proteins compared to results for the sample treated with TiO_2 at a concentration of 0.1 g/liter: outer membrane protein A (OmpA), spot 2; outer membrane protein C (OmpC), spot 3; outer membrane protein F (OmpF), spot 4; maltoporin (LamB), spot 6; a hypothetical protein, YggE, spot 8; a dipeptide binding protein (DppA), spot 9; an enoyl ACP reductase, (FabI), spot 11; Dps, spots 12 and 13; bacterioferritin (Bfr), spot 14; two-component response regulator (ArcA), spot 15; and a trigger factor (Tig), spot 17. These results indicate that TiO_2 alone induced a cytotoxic effect in the dark under our operating conditions.

The proteomic profile recorded after UV-A photocatalytic treatment for 30 min at the 0.1- and 0.4-g/liter TiO_2 concentrations are shown in Fig. 3D and Fig. 3F, respectively. Fourteen spots were missing in total at a TiO_2 concentration of 0.1 g/liter (Fig. 3D), among which 7 proteins (OmpA, spot 2; OmpC, spot 3; OmpF, spot 4; LamB, spot 6; YggE, spot 8; Bfr, spot 14; and ArcA, spot 15) are additional compared to results of the experiment performed in the dark in the presence of 0.1 g/liter TiO_2 (Fig. 3C). These proteins have already been identified in the sample treated solely with 0.4 g/liter TiO_2 (Fig. 3E). In contrast, the gel obtained from the sample irradiated during 30 min in the presence 0.4 g/liter of TiO_2 (Fig. 3F) showed only 3 additional disappearing proteins (putative nucleotide-binding protein [YajQ], spot 20; heat shock protein [GrpE], spot 21; and the HslV-HslU protein [protease HslV], spot 22) compared to results for the sample treated in the dark at a TiO_2 concentration of 0.4 g/liter (Fig. 3E). This result corresponds in total to 22 missing proteins.

DISCUSSION

It is well known that UV-A irradiation of TiO_2 induces production of ROS (33, 34). Generation of ROS is an unavoidable aspect of life under aerobic conditions, but the disruption of the balance between generation and elimination of ROS is reported to induce severe damage to important cell components, such as lipids, proteins, or nucleic acid (35, 36). Therefore, we have studied the influence of TiO_2 photocatalysis on lipids, which are one of the main compounds of the bacterial membrane. We performed this study in conjunction with studying the implication of ROS, by recording the amount of MDA—known to be the end product and main biomarker of lipid peroxidation (18, 37)—produced during the membrane alterations. The extent of lipid peroxidation induced by TiO_2 photocatalysis was in agreement with results shown by Maness et al. (18) and in the review by Dalrymple et al. (13). It was noteworthy that addition of SOD decreases by half the amount of lipid peroxidation products, confirming that $O_2{\cdot}^-$ is implicated in the lipid peroxidation process. However, we consider the possibility that other ROS, such as singlet oxygen $^1O_2$, can be generated from oxidation of $O_2{\cdot}^-$. This oxidation is thermodynamically favored since E^0 ($O_2{\cdot}^-/^1O_2$) = 0.34 V versus the normal hydrogen electrode (NHE) (38) and the formation of $^1O_2$ during photocatalysis on TiO_2 has been previously reported (39, 40) (E^0 is the standard redox potential). Consequently, we cannot exclude a potential involvement of $^1O_2$ in lipid peroxidation, knowing that the $^1O_2$ molecule is a highly energetic oxygen molecule known to lead to the initiation of lipid peroxidation reactions. This supports the direct implication of $O_2{\cdot}^-$ radicals as important active ROS in *E. coli* cell death, i.e., in the photocatalytic antimicrobial effect, as previously shown in G. Carré et al. (31).

The contact between *E. coli* bacterial cells and TiO_2, with or without UV-A irradiation, induced the disappearance of many spots. As shown in Table 1, the targeted proteins are very heterogeneous in cellular localization and belong to different function families. However, it is clear that most of the involved proteins belong to four main functional groups, porins (4/21), proteins involved in oxidative stress response (5/21), chaperone proteins (4/21), and to a lesser extent proteins involved in the transport and metabolism of different molecules. such as inorganic ions (2/21), lipids (2/21), carbohydrates (1/21), and

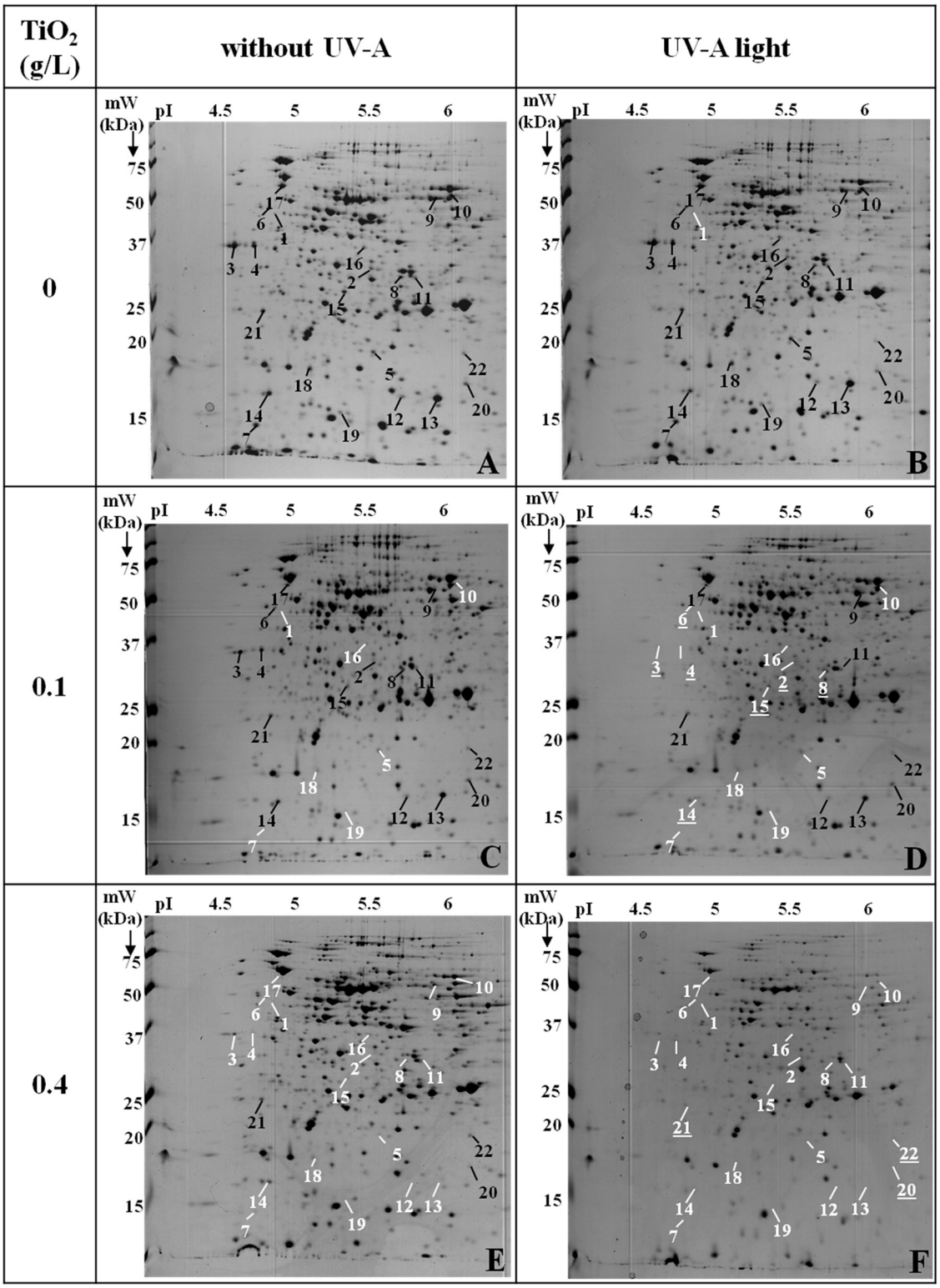

FIG 3 Impact of TiO_2 photocatalysis on the whole-cell proteome of *E. coli* ATCC 8739. Representative 2-DE gel pictures (pH range, 4 to 7) of whole-cell protein lysates after different treatments for 30 min of UV-A light irradiation are shown. Previously, bacteria were grown during 16 h to 18 h on tryptic soy agar at 37°C. (A) Standard conditions (without TiO_2 in the dark). (B) Under UV-A light irradiation. (C and E) In the dark at a TiO_2 concentration of 0.1 g/liter (C) or 0.4 g/liter (E). (D and F) Under UV-A light irradiation at a TiO_2 concentration of 0.1 g/liter (D) or 0.4 g/liter (F). Spots present (black numbers) under standard conditions (gel A) but not detected (white numbers) after one of the applied treatments (gels B to F) are shown. Proteins corresponding to these spots were identified by chip-LC-QTOF analysis.

TABLE 1 Identification of missing proteins in *E. coli* ATCC 8739 whole-cell proteomes recorded after 30 min of UV-A treatment, TiO_2 exposure in the dark, and a photocatalytic test

Functional category	Protein identity	Gene	Location	Spot no.	Peptides matched[a]	Coverage (%)	pI;[b] mW[c]	Treatment[d]
Lipid transport and metabolism	Unnamed protein product	*fadL*	Outer membrane	1	3/5	6	5.26; 42,307	UV; $C_{0.1}$; $C_{0.4}$
	Chain A, X-ray structure of *Escherichia coli* enoyl reductase with bound Nad and benzodiazaborine	*fabI*	Cytoplasm	11	15/18	43	5.58; 27,733	$C_{0.4}$
Porin	Outer membrane protein A	*ompA*	Outer membrane	2	11/12	24	5.99; 37,200	$P_{0.1}$; $C_{0.4}$
	Outer membrane porin protein C	*ompC*	Outer membrane	3	18/19	28	4.65; 41,447	$P_{0.1}$; $C_{0.4}$
	Outer membrane porin protein F	*ompF*	Outer membrane	4	18/18	29	4.82; 39,372	$P_{0.1}$; $C_{0.4}$
	Chain A, outer membrane protein OmpW	*ompW*	Outer membrane	5	6/6	10	6.15; 21,675	$C_{0.1}$; $C_{0.4}$
Carbohydrate transport and metabolism	Maltoporin	*lamB*	Outer membrane	6	7/9	10	4.86; 49,968	$P_{0.1}$; $C_{0.4}$
Amino acid transport and metabolism	Chain A, dipeptide-binding protein complex with glycyl-L-leucine	*dppA*	Inner membrane	9	23/29	24	5.74; 57,407	$C_{0.4}$
Inorganic ion transport and metabolism	DNA starvation/stationary-phase protection protein Dps	*dps*	Cytoplasm	12	52/54	61	5.70; 18,695	$C_{0.4}$
	DNA starvation/stationary-phase protection protein Dps	*dps*	Cytoplasm	13	52/54	61	5.70; 18,695	$C_{0.4}$
	Bacterioferritin, iron storage, and detoxification protein	*bfr*	Cytoplasm	14	24/24	69	4.69; 18,495	$P_{0.1}$; $C_{0.4}$
Energy production and conversion	H^+ ATPase F1 alpha subunit	*atpA*	Inner membrane	10	22/26	32	5,93; 55,339	$C_{0.1}$; $C_{0.4}$
Oxidative stress defense protein	Chain A, structure of the hypothetical protein YgiW	*ygiW*	Periplasm	7	14/15	45	4.73; 11,905	$C_{0.1}$; $C_{0.4}$
	Hypothetical protein ECP_2911	*yggE*	Periplasm	8	11/11	28	5.74; 24,981	$P_{0.1}$; $C_{0.4}$
	Two-component response regulator	*arcA*	Cytoplasm	15	12/14	35	5.20; 27,292	$P_{0.1}$; $C_{0.4}$
	Indigoidine synthase A-like protein	IndA-like protein gene	Cytoplasm	16	16/16	26	5.29; 32,921	$C_{0.1}$; $C_{0.4}$
	Putative nucleotide binding protein	*yajQ*	Cytoplasm	20	14/15	49	5.94; 18,312	$P_{0.4}$
Posttranslational modification, protein turnover, chaperones	Trigger factor	*tig*	Cytoplasm	17	65/70	56	4.73; 48,02	$C_{0.4}$
	DnaK suppressor	*dksA*	Cytoplasm	18	3/4	34	4,97; 17,500	$C_{0.1}$; $C_{0.4}$
	Heat shock protein GrpE	*grpE*	Cytoplasm	21	16/18	42	4.68; 21,741	$P_{0.4}$
	Chain A, HslV-HslU	Protease HslV gene	Cytoplasm	22	5/5	19	5.95; 18,962	$P_{0.4}$
Translation, ribosomal structure and biogenesis	Chain F	Ribosomal_S6	Cytoplasm	19	9/10	42	6.58; 11,164	$C_{0.1}$; $C_{0.4}$

[a] Peptides matched: number of tryptic peptides observed contributing to the percentage of sequence coverage with unique amino acid sequence/total number of unique peptides detected including posttranslational modifications.
[b] pI, theoretical isoelectric point.
[c] mW, theoretical molecular weight.
[d] Nature of the treatment leading to the disappearance of some proteins in 2-DE gels compared to results under standard conditions. UV, 30 min of UV-A irradiation; $C_{0.1}$ and $C_{0.4}$, treatment with a cytotoxic effect of TiO_2 at 0.1 g/liter and 0.4 g/liter, respectively; $P_{0.1}$ and $P_{0.4}$, photocatalytic treatment with TiO_2 at 0.1 g/liter and 0.4 g/liter, respectively.

amino acids (1/21). To a lesser extent, we also identified one protein involved in energy production and conversion, as well as one involved in translation regulation.

The disappearance of a spot during the applied treatment in comparison with the control gel may reflect a denaturation, a cleavage, an oxidation, or a change in the location of the spot on the gel. However, we must consider that different functional protein isoforms may be present in the proteome, such as Omp proteins, located at the outer membrane. In the case of OmpA (spot 2), many isoforms of this protein are described in the literature, with 8 already reported in the sole publication of Molloy et al. (41). Thus, the alteration of a spot does not necessarily mean that the protein is no longer functional. Even if no direct information on the proteomic functionality can be obtained, this proteomic analysis identifies potential proteins that are affected by cytotoxic treatment in the dark with TiO_2 and by a photocatalytic treatment in the presence of UV-A-light-irradiated TiO_2.

Taking into account the criteria relative to the presence or absence of a spot in comparison with the control gel, the modification of a selected spot should be correlated to the appearance of another spots in the gel corresponding to the same protein. However, presence/absence comparative analysis did not reveal the appearance of any new spots in the gels. Therefore, we can assume that the spots that have been altered have led to the formation of new, undetectable spots. This can be explained by three nonexclusive hypotheses: (i) the cleavage of the protein can result in the formation of spots too small to be observed in the gel (smaller than 10 kDa), (ii) spots corresponding to proteins with a pH out of the observation range of the gel (i.e., outside the 4 to 7 pH range) may be present, and (iii) the new spots may be superimposed on the

gels with initially present spots. The disappearance of spots is most likely due to oxidative degradation of proteins and cannot be attributed to regulation of protein expression as an answer to oxidative stress. Indeed, oxidation reactions and protease activity to degrade proteins are fast (42), and while the applied treatments may be long enough (30 min) to cause transcriptional events for the genes encoding the identified proteins, this time is too short for efficient protein translation (43). In fact, we precisely chose these conditions so as not to observe genome-based protein regulation phenomena.

We showed that these alterations were not specific to any functional class, although some proteins, such as outer membrane proteins, were the main target during the treatment with TiO_2 in the dark and with photocatalytic treatment with TiO_2 in the presence of UV-A irradiation, probably due to their direct contact with TiO_2 particles. In particular, it is reported that about 70% of the surface of the membrane of Gram-negative bacteria is composed of porins. Their role is to allow the passage of nutrients and in particular the permeation of hydrophilic molecules (44). Some of them, OmpA and OmpC especially, have already been identified as the main targets when *E. coli* cells are exposed to external oxidative stress (45). Recently, Krishnan and Prasadarao have shown that OmpA, which is a multifunctional major outer membrane protein of *E. coli* and the *Enterobacteriaceae*, interacts with specific receptors, initiating the pathogenesis of some Gram-negative bacterial infections (46). We hypothesized that the degradation of these mains OMPs by both the cytotoxic effect of TiO_2 and the ROS generated by the photocatalytic reaction on TiO_2 disrupts the communication between bacteria and the environment.

Five protein spots corresponding to oxidative stress proteins were also altered by both cytotoxic and photo catalytic effect of TiO_2. These include two proteins located in the periplasm (YgiW and YggE) and three others located in the cytoplasm (ArcA, IndA-like, and YajQ). The cytoplasmic YajQ protein was the single additional protein modified only during UV-A photocatalysis and not with TiO_2 in the dark, in comparison to the others, which were already modified in the dark (TiO_2 cytotoxic effect). The YggE gene product is involved in the reduction of the intracellular ROS level and is therefore responsible for lowering the concentration of ROS to a tolerated level (47). ArcA is a two-component response regulator involved in the oxidative stress response (48, 49), and YajQ is involved in ROS detoxification mechanism (50).

Members of the chaperone protein family are also altered, since we found the disappearance of 2 proteins (Tig and DksA) when studying the TiO_2 cytotoxic effect and 2 others (GrpE and protease HslV) during the photocatalytic effect at 0.4 g/liter of TiO_2. The GrpE heat shock protein in interaction with DnaK and DnaJ can prevent the aggregation of stress-denatured proteins (51), and HslV is an ATP-dependent protease, which helps in the degradation of denatured proteins (52).

Proteins involved in transport and metabolism, crucial for bacterial survival and growth, are also altered. Cytotoxicity of 0.4 g/liter TiO_2 caused the disappearance of three spots, assigned to two Dps isoforms and Bfr, which are responsible for inorganic ion transport and metabolism. The Dps protein protects DNA from damage resulting from oxidative stress. This protection is performed by sequestering and mineralizing metal ions, especially ferrous ion, that can be engaged in the Fenton reaction and are known to yield hydroxyl radicals that can damage macromolecules, such as proteins, membrane lipids. and DNA (20, 53–55). We have noted that the cytotoxic effect at s TiO_2 concentration of 0.4 g/liter induced the disappearance of two isoforms of this protein (spots 12 and 13). The second protein is Bfr, which is a bacterioferritin and has specific detoxifying properties for the damaging action of ROS (56).

Small ribosomal proteins were also altered by the cytotoxic effect of TiO_2. We have observed the disappearance of the spot corresponding to ribosomal S6. Protein S6 is located in the central domain of the small ribosomal subunit, and the level of this small ribosomal protein S6 could be modified by the induction of the *soxRS* regulon (SoxR being identified as a sensor for superoxide anions) (35). However, it was shown that *E. coli* strains with in-frame deletions of the S6 ribosomal protein are still viable and show no deficiency of 30S protein composition (57).

Although no information about metabolism regulation during photocatalytic treatment can be derived from the 2-DE analysis, we suggested that protein modification could disrupt the ability of the bacteria to communicate with the environment.

We hypothesized that such potential protein alteration and lipid peroxidation participated in the antibacterial activity which occurred during the UV-A photocatalytic treatment with TiO_2. For this study, demonstrating the impact of UV-A photocatalysis with TiO_2 on the proteome of *E. coli*, we selected a qualitative analysis in order to identify the protein spots that are significantly affected (presence versus absence) by the different treatments applied. Twenty-two proteins are surely few, and many more are certainly modified, but this approach allowed us to demonstrate that the different altered spots belong to several protein function categories. The hypothesis that all the *E. coli* proteins could be affected without any important selectivity during photocatalysis, as previously suggested by Goulhen-Chollet et al. (19), could now be supported by our observation, since the proteins altered by UV-A photocatalysis with TiO_2 belong to several functional categories, with a majority of them being involved in oxidative stress and porins. The proteomic approach was informative for identifying the proteins altered in the antibacterial process taking place with TiO_2 nanoparticles and may ultimately be used to determine how their expression is controlled. Further work will concern comparative genomic/transcriptomic/proteomic analyses, e.g., performed with mutant strains, to gain more insights into the development of molecular mechanisms of bacterial resistance to UV-A photocatalysis with TiO_2, which could occur in bacteria containing a different enzymatic/proteomic arsenal.

Conclusions. The present study has identified the effects of UV-A photocatalysis with TiO_2 and those of TiO_2 in the dark on key cellular components of *E. coli*, such as lipid and proteins. It showed that antibacterial photocatalytic activity was accompanied by lipid peroxidation resulting from the reaction with the $O_2^{\cdot -}$ superoxide radical ROS. This lipid peroxidation could enhance membrane fluidity and disrupt cell integrity. The 2-DE proteomic analysis is the first study to gain insight into the antimicrobial effect of TiO_2 photocatalysis by focusing on the identification of potential protein targets modified during the cytotoxic treatment in the dark with TiO_2 and the TiO_2 photocatalytic treatment in the presence of UV-A irradiation. The mass spectrometry protein analysis has shown that the protein alterations were not specific to a functional class, although some proteins, such as outer membrane proteins, were the main target during both treatments, probably as a result of a greater exposure to the surface of TiO_2

particles. The main degraded proteins were porins and proteins mainly involved in the response to oxidative stress or in environmental stress regulation.

ACKNOWLEDGMENTS

We are grateful to DGA (Direction Générale de l'Armement) and the Alsace regional council for funding the Ph.D. grant for Gaëlle Carré.

Nicole Glasser is thanked for her contribution to statistical analysis.

REFERENCES

1. **Silvestry-Rodriguez N, Sicairos-Ruelas EE, Gerba CP, Bright KR.** 2007. Silver as a disinfectant. Rev. Environ. Contam. Toxicol. **191:**23–45. http://dx.doi.org/10.1007/978-0-387-69163-3_2.
2. **Ruparelia JP, Chatterjee AK, Duttagupta SP, Mukherji S.** 2008. Strain specificity in antimicrobial activity of silver and copper nanoparticles. Acta Biomater. **4:**707–716. http://dx.doi.org/10.1016/j.actbio.2007.11.006.
3. **Wolska KI, Grzes K, Kurek A.** 2012. Synergy between novel antimicrobials and conventional antibiotics or bacteriocins. Pol. J. Microbiol. **61:**95–104.
4. **Borkow G, Gabbay J.** 2005. Copper as a biocidal tool. Curr. Med. Chem. **12:**2163–2175. http://dx.doi.org/10.2174/0929867054637617.
5. **Silver S, Phung LT.** 1996. Bacterial heavy metal resistance: new surprises. Annu. Rev. Microbiol. **50:**753–789. http://dx.doi.org/10.1146/annurev.micro.50.1.753.
6. **Malato S, Fernandez-Ibanez P, Maldonado MI, Blanco J, Gernjak W.** 2009. Decontamination and disinfection of water by solar photocatalysis: recent overview and trends. Catal. Today **147:**1–59. http://dx.doi.org/10.1016/j.cattod.2009.06.018.
7. **Matsunaga T, Tomoda R, Nakajima T, Wake H.** 1985. Photoelectrochemical sterilization of microbial cells by semiconductor powders. FEMS Microbiol. Lett. **29:**211–214. http://dx.doi.org/10.1111/j.1574-6968.1985.tb00864.x.
8. **Wei C, Lin WY, Zainal Z, Williams NE, Zhu K, Kruzic AP, Smith RL, Rajeshwar K.** 1994. Bactericidal activity of TiO_2 photocatalyst in aqueous media: toward a solar-assisted water disinfection system. Environ. Sci. Technol. **28:**934–938. http://dx.doi.org/10.1021/es00054a027.
9. **Gelover S, Gomez LA, Reyes K, Teresa Leal M.** 2006. A practical demonstration of water disinfection using TiO2 films and sunlight. Water Res. **40:**3274–3280. http://dx.doi.org/10.1016/j.watres.2006.07.006.
10. **Ede S, Hafner L, Dunlop P, Byrne J, Will G.** 2012. Photocatalytic disinfection of bacterial pollutants using suspended and immobilized TiO_2 powders. Photochem. Photobiol. **88:**728–735. http://dx.doi.org/10.1111/j.1751-1097.2012.01104.x.
11. **Carp O, Huisman CL, Reller A.** 2004. Photoinduced reactivity of titanium dioxide. Prog. Solid State Chem. **32:**33–177. http://dx.doi.org/10.1016/j.progsolidstchem.2004.08.001.
12. **Foster HA, Ditta IB, Varghese S, Steele A.** 2011. Photocatalytic disinfection using titanium dioxide: spectrum and mechanism of antimicrobial activity. Appl. Microbiol. Biotechnol. **90:**1847–1868. http://dx.doi.org/10.1007/s00253-011-3213-7.
13. **Dalrymple OK, Stefanakos E, Trotz MA, Goswami DY.** 2010. A review of the mechanisms and modeling of photocatalytic disinfection. Appl. Catal. B Environ. **98:**27–38. http://dx.doi.org/10.1016/j.apcatb.2010.05.001.
14. **Josset S, Keller N, Lett MC, Ledoux MJ, Keller V.** 2008. Numeration methods for targeting photoactive materials in the UV-A photocatalytic removal of microorganisms. Chem. Soc. Rev. **37:**744–755. http://dx.doi.org/10.1039/b711748p.
15. **Cho M, Chung H, Choi W, Yoon J.** 2005. Different inactivation behaviors of MS-2 phage and *Escherichia coli* in TiO_2 photocatalytic disinfection. Appl. Environ. Microbiol. **71:**270–275. http://dx.doi.org/10.1128/AEM.71.1.270-275.2005.
16. **Robertson PK, Robertson JM, Bahnemann DW.** 2012. Removal of microorganisms and their chemical metabolites from water using semiconductor photocatalysis. J. Hazard. Mater. **211–212:**161–171. http://dx.doi.org/10.1016/j.jhazmat.2011.11.058.
17. **Gogniat G, Thyssen M, Denis M, Pulgarin C, Dukan S.** 2006. The bactericidal effect of TiO_2 photocatalysis involves adsorption onto catalyst and the loss of membrane integrity. FEMS Microbiol. Lett. **258:**18–24. http://dx.doi.org/10.1111/j.1574-6968.2006.00190.x.
18. **Maness PC, Smolinski S, Blake DM, Huang Z, Wolfrum EJ, Jacoby WA.** 1999. Bactericidal activity of photocatalytic TiO_2 reaction: toward an understanding of its killing mechanism. Appl. Environ. Microbiol. **65:**4094–4098.
19. **Goulhen-Chollet F, Josset S, Keller N, Keller V, Lett M-C.** 2009. Monitoring the bactericidal effect of UV-A photocatalysis: a first approach through 1D and 2D protein electrophoresis. Catal. Today **147:**169–172. http://dx.doi.org/10.1016/j.cattod.2009.06.001.
20. **Gogniat G, Dukan S.** 2007. TiO2 photocatalysis causes DNA damage via Fenton reaction-generated hydroxyl radicals during the recovery period. Appl. Environ. Microbiol. **73:**7740–7743. http://dx.doi.org/10.1128/AEM.01079-07.
21. **Huang Z, Maness P-C, Blake DM, Wolfrum EJ, Smolinski SL, Jacoby WA.** 2000. Bactericidal mode of titanium dioxide photocatalysis. J. Photochem. Photobiol. A Chem. **130:**163–170. http://dx.doi.org/10.1016/S1010-6030(99)00205-1.
22. **Gumy D, Morais C, Bowen P, Pulgarin C, Giraldo S, Hajdu R, Kiwi J.** 2006. Catalytic activity of commercial of TiO_2 powders for the abatement of the bacteria (*E. coli*) under solar simulated light: influence of the isoelectric point. Appl. Catal. B Environ. **63:**76–84. http://dx.doi.org/10.1016/j.apcatb.2005.09.013.
23. **Vacaroiu C, Enache M, Gartner M, Popescu G, Anastasescu M, Brezeanu A, Todorova N, Giannakopoulou T, Trapalis C, Dumitru L.** 2009. The effect of thermal treatment on antibacterial properties of nanostructured TiO_2(N) films illuminated with visible light. World J. Microbiol. Biotechnol. **25:**27–31. http://dx.doi.org/10.1007/s11274-008-9856-6.
24. **Pigeot-Rémy S, Simonet F, Errazuriz-Cerda E, Lazzaroni JC, Atlan D, Guillard C.** 2011. Photocatalysis and disinfection of water: identification of potential bacterial targets. Appl. Catal. B Environ. **104:**390–398. http://dx.doi.org/10.1016/j.apcatb.2011.03.001.
25. **Lukjancenko O, Wassenaar TM, Ussery DW.** 2010. Comparison of 61 sequenced *Escherichia coli* genomes. Microb. Ecol. **60:**708–720. http://dx.doi.org/10.1007/s00248-010-9717-3.
26. **Hamon E, Horvatovich P, Izquierdo E, Bringel F, Marchioni E, Aoude-Werner D, Ennahar S.** 2011. Comparative proteomic analysis of *Lactobacillus plantarum* for the identification of key proteins in bile tolerance. BMC Microbiol. **11:**63. http://dx.doi.org/10.1186/1471-2180-11-63.
27. **Geer LY, Markey SP, Kowalak JA, Wagner L, Xu M, Maynard DM, Yang X, Shi W, Bryant SH.** 2004. Open mass spectrometry search algorithm. J. Proteome Res. **3:**958–964. http://dx.doi.org/10.1021/pr0499491.
28. **Kapp EA, Schutz F, Connolly LM, Chakel JA, Meza JE, Miller CA, Fenyo D, Eng JK, Adkins JN, Omenn GS, Simpson RJ.** 2005. An evaluation, comparison, and accurate benchmarking of several publicly available MS/MS search algorithms: sensitivity and specificity analysis. Proteomics **5:**3475–3490. http://dx.doi.org/10.1002/pmic.200500126.
29. **Herrmann JM.** 1999. Heterogeneous photocatalysis: fundamentals and applications to the removal of various types of aqueous pollutants. Catal. Today **53:**115–129. http://dx.doi.org/10.1016/S0920-5861(99)00107-8.
30. **Herrmann JM.** 2005. Heterogeneous photocatalysis: state of the art and present applications. Top. Catal. **34:**49–65. http://dx.doi.org/10.1007/s11244-005-3788-2.
31. **Carre G, Benhamida D, Peluso J, Muller CD, Lett MC, Gies JP, Keller V, Keller N, Andre P.** 2013. On the use of capillary cytometry for assessing the bactericidal effect of TiO_2. Identification and involvement of reactive oxygen species. Photochem. Photobiol. Sci. **12:**610–620. http://dx.doi.org/10.1039/c2pp25189b.
32. **Oliver JD, Dagher M, Linden K.** 2005. Induction of *Escherichia coli* and *Salmonella typhimurium* into the viable but nonculturable state following chlorination of wastewater. J. Water Health **3:**249–257.
33. **Hoffmann MR, Martin ST, Choi W, Bahnemann DW.** 1995. Environmental applications of semiconductor photocatalysis. Chem. Rev. **95:**69–96. http://dx.doi.org/10.1021/cr00033a004.
34. **Ma H, Brennan A, Diamond SA.** 2012. Photocatalytic reactive oxygen species production and phototoxicity of titanium dioxide nanoparticles are dependent on the solar ultraviolet radiation spectrum. Environ. Toxicol. Chem. **31:**2099–2107. http://dx.doi.org/10.1002/etc.1916.
35. **Lushchak VI.** 2011. Adaptive response to oxidative stress: bacteria, fungi, plants and animals. Comp. Biochem. Physiol. C Toxicol. Pharmacol. **153:**175–190. http://dx.doi.org/10.1016/j.cbpc.2010.10.004.
36. **Mitoraj D, Janczyk A, Strus M, Kisch H, Stochel G, Heczko PB, Macyk W.** 2007. Visible light inactivation of bacteria and fungi by modified titanium dioxide. Photochem. Photobiol. Sci. **6:**642–648. http://dx.doi.org/10.1039/b617043a.
37. **Kohen R, Nyska A.** 2002. Oxidation of biological systems: oxidative

stress phenomena, antioxidants, redox reactions, and methods for their quantification. Toxicol. Pathol. **30:**620–650. http://dx.doi.org/10.1080/01926230290166724.
38. **Sawyer DT.** 1981. How super is superoxide? Acc. Chem. Res. **14:**393–400. http://dx.doi.org/10.1021/ar00072a005.
39. **Daimon T, Hirakawa T, Kitazawa M, Suetake J, Nosaka Y.** 2008. Formation of singlet molecular oxygen associated with the formation of superoxide radicals in aqueous suspensions of TiO_2 photocatalysts. Appl. Catal. A Gen. **340:**169–175. http://dx.doi.org/10.1016/j.apcata.2008.02.012.
40. **Rengifo-Herrera JA, Pierzchala K, Sienkiewicz A, Forro L, Kiwi J, Pulgarin C.** 2009. Abatement of organics and *Escherichia coli* by N,S co-doped TiO_2 under UV and visible light. Implications of the formation of singlet oxygen ($^1O_2$) under visible light. Appl. Catal. B Environ. **88:**398–406. http://dx.doi.org/10.1016/j.apcatb.2008.10.025.
41. **Molloy MP, Herbert BR, Slade MB, Rabilloud T, Nouwens AS, Williams KL, Gooley AA.** 2000. Proteomic analysis of the *Escherichia coli* outer membrane. Eur. J. Biochem. **267:**2871–2881. http://dx.doi.org/10.1046/j.1432-1327.2000.01296.x.
42. **Krämer R.** 2010. Bacterial stimulus perception and signal transduction: response to osmotic stress. Chem. Rec. **10:**217–229. http://dx.doi.org/10.1002/tcr.201000005.
43. **Golding I, Paulsson J, Zawilski SM, Cox EC.** 2005. Real-time kinetics of gene activity in individual bacteria. Cell **123:**1025–1036. http://dx.doi.org/10.1016/j.cell.2005.09.031.
44. **Jaroslawski S, Duquesne K, Sturgis J, Scheuring S.** 2009. High-resolution architecture of the outer membrane of the Gram-negative bacteria *Roseobacter denitrificans*. Mol. Microbiol. **74:**1211–1222. http://dx.doi.org/10.1111/j.1365-2958.2009.06926.x.
45. **Tamarit J, Cabiscol E, Ros J.** 1998. Identification of the major oxidatively damaged proteins in *Escherichia coli* cells exposed to oxidative stress. J. Biol. Chem. **273:**3027–3032. http://dx.doi.org/10.1074/jbc.273.5.3027.
46. **Krishnan S, Prasadarao NV.** 2012. Outer membrane protein A and OprF: versatile roles in Gram negative bacterial infections. FEBS J. **279:**919–931. http://dx.doi.org/10.1111/j.1742-4658.2012.08482.x.
47. **Kim SY, Nishioka M, Hayashi S, Honda H, Kobayashi T, Taya M.** 2005. The gene *yggE* functions in restoring physiological defects of *Escherichia coli* cultivated under oxidative stress conditions. Appl. Environ. Microbiol. **71:**2762–2765. http://dx.doi.org/10.1128/AEM.71.5.2762-2765.2005.
48. **Lu S, Killoran PB, Fang FC, Riley LW.** 2002. The global regulator ArcA controls resistance to reactive nitrogen and oxygen intermediates in *Salmonella enterica* serovar Enteritidis. Infect. Immun. **70:**451–461. http://dx.doi.org/10.1128/IAI.70.2.451-461.2002.
49. **Kohanski MA, Dwyer DJ, Wierzbowski J, Cottarel G, Collins JJ.** 2008. Mistranslation of membrane proteins and two-component system activation trigger antibiotic-mediated cell death. Cell **135:**679–690. http://dx.doi.org/10.1016/j.cell.2008.09.038.
50. **Amitai S, Kolodkin-Gal I, Hananya-Meltabashi M, Sacher A, Engelberg-Kulka H.** 2009. *Escherichia coli* MazF leads to the simultaneous selective synthesis of both "death proteins" and "survival proteins". PLoS Genet. **5:**e1000390. http://dx.doi.org/10.1371/journal.pgen.1000390.
51. **Harrison C.** 2003. GrpE, a nucleotide exchange factor for DnaK. Cell Stress Chaperones **8:**218–224. http://dx.doi.org/10.1379/1466-1268(2003)008<0218:GANEFF>2.0.CO;2.
52. **Lau-Wong IC, Locke T, Ellison MJ, Raivio TL, Frost LS.** 2008. Activation of the Cpx regulon destabilizes the F plasmid transfer activator, TraJ, via the HslVU protease in *Escherichia coli*. Mol. Microbiol. **67:**516–527. http://dx.doi.org/10.1111/j.1365-2958.2007.06055.x.
53. **Nair S, Finkel SE.** 2004. Dps protects cells against multiple stresses during stationary phase. J. Bacteriol. **186:**4192–4198. http://dx.doi.org/10.1128/JB.186.13.4192-4198.2004.
54. **Yellaboina S, Ranjan S, Chakhaiyar P, Hasnain SE, Ranjan A.** 2004. Prediction of DtxR regulon: identification of binding sites and operons controlled by Diphtheria toxin repressor in *Corynebacterium diphtheriae*. BMC Microbiol. **4:**38. http://dx.doi.org/10.1186/1471-2180-4-38.
55. **Liu X, Theil EC.** 2005. Ferritins: dynamic management of biological iron and oxygen chemistry. Acc. Chem. Res. **38:**167–175. http://dx.doi.org/10.1021/ar0302336.
56. **Chiancone E, Ceci P, Ilari A, Ribacchi F, Stefanini S.** 2004. Iron and proteins for iron storage and detoxification. Biometals **17:**197–202. http://dx.doi.org/10.1023/B:BIOM.0000027692.24395.76.
57. **Shajani Z, Sykes MT, Williamson JR.** 2011. Assembly of bacterial ribosomes. Annu. Rev. Biochem. **80:**501–526. http://dx.doi.org/10.1146/annurev-biochem-062608-160432.